Study of Wild Type and Genetically Modified Reaction Centers from *Rhodobacter capsulatus*: Structural Comparison with *Rhodopseudomonas viridis* and *Rhodobacter sphaeroides*

Laura Baciou,* Edward J. Bylina,‡ and Pierre Sebban*

*UPR 407, Bat. 24, Centre National de le Recherche Scientifique Gif/Yvette, 91198, France; ‡University of Hawaii at Manoa, Biotechnology Program, Pacific Biomedical Research Center, Honolulu, Hawaii 96822 USA

ABSTRACT Reaction centers from the purple bacterium *Rhodobacter* (*Rb.*) *capsulatus* and from two mutants $Thr^{L226} \rightarrow Ala$ and $Ile^{L229} \rightarrow Ser$, modified in the binding protein pocket of the secondary quinone acceptor (Q_B), have been studied by flash-induced absorbance spectroscopy. In $Thr^{L226} \rightarrow Ala$, the binding affinities for endogenous Q_B (ubiquinone 10) and UQ_6 are found to be two to three times as high as in the wild type. In contrast, in $Ile^{L229} \rightarrow Ser$, the binding affinity for UQ_6 is decreased about three times compared to the wild type. In $Thr^{L226} \rightarrow Ala$, a markedly increased sensitivity (~30 times) to *o*-phenanthroline is observed. In *Rhodopseudomonas viridis*, where Ala is naturally in position L226, the sensitivity to *o*-phenanthroline is close to that observed in $Thr^{L226} \rightarrow Ala$. We propose that the presence of Ala in position L226 is responsible for the high sensitivity to that inhibitor. The pH dependencies of the rate constants of $P^+Q_B^-$ (k_{BP}) charge recombination kinetics (*P* is a dimer of bacteriochlorophyll, and Q_B is the secondary quinone electron acceptor) show destabilization of Q_B^- in $Thr^{L226} \rightarrow Ala$ and $Ile^{L229} \rightarrow Ser$, compared to the wild type. At low pH, similar apparent pK values of protonation of amino acids around Q_B^- are measured in the wild type and the mutants. In contrast to *Rb. sphaeroides*, in the wild type *Rb. capsulatus*, k_{BP} substantially increases in the pH range 7–10. This may reflect some differences in the respective structures of both strains or, alternatively, may be due to deprotonation of Tyr^{L215} in *Rb. capsulatus*. At pH 7, measurements of the rate constant of Q_A^- to Q_B electron transfer reveal a threefold greater rate in the reaction centers from wild type *Rb. capsulatus* $(65 \pm 10\,\mu s)^{-1}$ compared to *Rb. sphaeroides*. We suggest that this may arise from a 0.7-Å smaller distance between the quinones in the former strain. Our spectroscopic data on the wild type *Rb. capsulatus* reaction center suggest the existence of notable differences with the *Rb. sphaeroides* reaction center structure.

INTRODUCTION

Photosynthetic reaction centers convert light excitation energy into chemical free energy. The first step is achieved through a transmembrane charge separation. Bacterial reaction centers are composed of three polypeptides, L, M, and H with molecular masses ranging between 30 and 35 kDa. The primary electron donor is a dimer of bacteriochlorophyll, *P*. The first stable transmembrane charge separation occurs between *P* and Q_A, the first quinone electron acceptor which is located in a hydrophobic pocket provided by the M subunit. Q_A, which is a one-electron carrier, reduces the second quinone acceptor, Q_B, in 20–200 μs depending on the bacterial species. Q_B binds to a relatively polar protein domain located in the L subunit and works as a two-electron acceptor. Q_B^- is tightly bound to the reaction center (1). In contrast, Q_B is loosely bound in the fully reduced form which leaves the reaction center in the quinol state, Q_BH_2, after two protons have been taken up from the cytoplasmic side of the protein (2).

Q_B can be displaced from its binding site by competitive inhibitors (herbicides) which bind in the same protein pocket (1). Herbicide-resistant mutants from different bacterial species have been either designed by site-directed mutagenesis or isolated through their ability to grow in the presence of herbicides. This was done for *Rb. capsulatus* (3), *Rb. sphaeroides* (4), and *Rps. viridis* (5). All these mutants are modified in the primary sequence of the Q_B binding pocket. It has been pointed out that the replacement of Ile^{L229} in *Rb. sphaeroides* and *Rb. capsulatus* is of special interest. From the three-dimensional structure of the reaction centers from *Rb. sphaeroides* (6–8), van der Waals contacts are likely to exist between that residue and Q_B. Depending on the nature of the substitution in *Rb. capsulatus*, mutations in the Q_B pocket lead to varying levels of photosynthetic growth (9). From the three-dimensional structure of the reaction center from *Rps. viridis* (10) with the *s*-triazine herbicide terbutryn bound in the Q_B pocket, it appears that Ile^{L229} also develops extensive van der Waals contacts with this inhibitor. Another interesting *Rb. capsulatus* mutant is $Thr^{L226} \rightarrow Ala$ (9). Ala is naturally in the L226 position in *Rps. viridis*. We have studied reaction centers from the two mutants $Thr^{L226} \rightarrow Ala$ and $Ile^{L229} \rightarrow Ser$ from *Rb. capsulatus* with respect to their binding affinities for Q_B, *o*-phenanthroline, and terbutryn. Spectroscopic data are sparse for electron transfer reactions involving the quinones in *Rb. capsulatus* reaction centers. Thus, in order to study the energetics of the quinone system, the pH dependencies of the rates of $P^+Q_A^-$ and $P^+Q_B^-$ charge recombination as well as the Q_A^- to Q_B electron transfer rates were measured in the wild type and the mutants. The deduced quinone energetics are compared to those in *Rb. sphaeroides*.

MATERIALS AND METHODS

The wild type and mutant cultures were grown semiaerobically in the dark. $Ile^{L229} \rightarrow Ser$ and $Thr^{L226} \rightarrow Ala$ *Rb. capsulatus* mutants were produced by site-directed mutagenesis and isolated by resistance to atrazine, respectively

Received for publication 20 April 1992 and in final form 9 April 1993.

0006-3495/93/08/652/09 $2.00

(9). Isolation of the reaction centers from the wild type and mutants was achieved as follows. The cells were passed twice through a French press (~16,000 psi) in 0.1 M sodium phosphate, pH 7.5, and spun for 1 h at 20,000 *g*. The supernatant was spun again at ~100,000 *g* for 3 h. The pellets containing the membranes were then washed in 10 mM sodium phosphate, pH 7.5, 0.05% LDAO. Chromatophores were diluted in the same buffer to an optical density of about 8 at 875 nm. Detergent solubilization was achieved at 35–36°C, in the dark, by incubation with 1% LDAO, for 10 min. The solution was immediately cooled on ice and spun for 90 min. at 120,000 *g*. Reaction centers were largely contained in the supernatant, but were sometimes still present in the pellet. If so, a 1.5% LDAO solubilization followed by another 90-min spin was then necessary to further solubilize the reaction centers. The reaction center solution was then mixed with the same volume of DEAE-Sepharose equilibrated in 10 mM sodium phosphate, pH 7.5, LDAO 0.05%, 100 μM EDTA. The gel was then poured into a column, and washed with a step NaCl gradient. Reaction centers were eluted at 175 mM NaCl. When necessary, the DEAE column step was repeated to further purify the preparation.

UQ_6 was obtained from Sigma Chemical Co. (St. Louis, MO). pH buffers used were 2-(*N*-morpholino)ethanesulfonic acid (MES) (Sigma) between pH 5.5 and 6.5; 1,3-bis[tris(hydroxymethyl)methylamino]propane) (bis-Tris propane) (Sigma) between pH 6.3 and 9.5; 3-(cyclohexylamino)-propanesulfonic acid (CAPS) (Calbiochem) above pH 9.5.

The UQ_{10}, UQ_6, and *o*-phenanthroline titration curves were fitted according to a Marquardt algorithm by using the "Multifit" Macintosh program. The exponential decompositions of the charge recombination kinetics were achieved with a home-made program using the same algorithm.

RESULTS

Q_B binding affinities

The binding of Q_B in the reaction centers is described by the equilibrium:

$$[RC] + [Q] \overset{K_M}{<\!\!-\!\!>} [RC]_{QB} \quad (1)$$

where K_M represents the dissociation constant for Q_B. $[RC]$, $[Q]$, and $[RC]_{QB}$ are the respective concentrations of free reaction centers, free quinones, and reaction centers with bound Q_B. In the titration experiments described below, $[RC]$ and $[Q]$ substantially differ from their total values ($[RC]_{total}$ and $[Q]_{total}$, respectively). This is taken into account in Eq. 2 which describes the amount of Q_B site activity, $\%Q_B$, measured by the extent of the amplitude of $P^+Q_B^-$ charge recombination. In this equation $r = [Q]_{total}/[RC]_{total}$.

$$\%Q_B = \frac{[RC]_{Q_B}}{[RC]_{total}} = \frac{\left[1 + r + \frac{K_M}{[RC]_{total}}\right] - \left\{\left[1 + r + \frac{K_M}{[RC]_{total}}\right]^2 - 4r\right\}^{1/2}}{2} \quad (2)$$

Endogenous UQ_{10} titrations in the wild type and Thr^{L226} → Ala

As measured from the relative amplitude of the slow phase ($P^+Q_B^-$) of the charge recombination decay kinetics (not shown), the reaction center preparations (~7 μM) from the wild type and the Thr^{L226} → Ala mutant contained about 70–75% of residual Q_B activity. The residual Q_B activity measured in the Ile^{L229} → Ser mutant was much lower (<15%). The dissociation constants for the native Q_B were determined in the reaction centers from the wild type and the Thr^{L226} → Ala mutant. In concentrated reaction center preparations (~35 μM), we have determined by quinone extraction (11) the amount, *r*, of quinone per reaction center. The *r* value was estimated by two independent assays and was equal to 2.50 ± 0.05. This value corresponds to 1.50 ± 0.05 Q_B molecule present in the solution per reaction center. Assuming this ratio, we have titrated $\%Q_B$ vs. $[RC]_{total}$ for the wild type and the Thr^{L226} → Ala mutant, by diluting the reaction center stock solutions. These titrations are presented in Fig. 1. The fitting of these curves was achieved by using Eq. 2. A rough estimation of the K_M values for native UQ_{10} is then obtained: for the wild type, K_M = 0.71 ± 0.20 μM, for the Thr^{L226} → Ala mutant, K_M = 0.38 ± 0.15 μM (Table 1). Thus, the affinity for endogenous quinone is increased in the Thr^{L226} → Ala mutant compared to the wild type.

When *r* is not fixed in the above fitting procedure, in the range of reaction center concentrations used in these experiments, the *r* value does not vary much and stays in the range 1–1.5. The error bars given in the K_M values take into account these variations.

UQ_6 titrations

The dissociation constant values for exogenous UQ_6 were determined from the titration curves of $\%Q_B$ vs. $[UQ_6]$ (added quinone), in the wild type and the two mutants (Fig. 2). These curves were basically fitted by the model described in Eq. 2. However, even at high quinone concentration (≥ 100 μM), the asymptote value to which $\%Q_B$ tends is not 100%. The limit is about 90% for the wild type and Thr^{L226} → Ala,

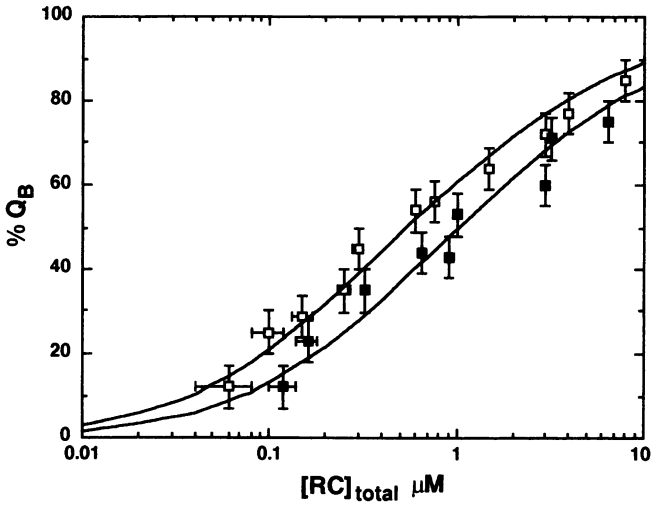

FIGURE 1 Titrations of the secondary quinone activity as measured from the relative amplitude of the slow phase of charge recombination measured at 865 nm on a home-made spectrophotometer; (■) in reaction centers from the wild type, (□) in the reaction centers from the Thr^{L226} → Ala mutant. Titrations were performed by dilution of the reaction center preparations. The lines are drawn by fitting the data with the model described in Eq. 2. This analysis leads to K_M values of 0.71 ± 0.15 μM for the wild type and 0.38 ± 0.15 μM for the Thr^{L226} → Ala mutant. The reaction centers were suspended in sodium phosphate, 10 mM, pH 7.5, LDAO 0.05%. T = 21°C.

TABLE 1 Dissociation constants (μM) for ubiquinones and *o*-phenanthroline in the wild type *Rb. capsulatus*, $Thr^{L226} \rightarrow$ Ala, and $Ile^{L229} \rightarrow$ Ser mutants

	K_M, endogenous UQ_{10}	K_M, UQ_6	K_i, *o*-phenanthroline
Wild type	0.71 ± 0.20	2.10 ± 0.30	166 ± 10
$Thr^{L226} \rightarrow$ Ala	0.38 ± 0.15	0.70 ± 0.15	5 ± 2
$Ile^{L229} \rightarrow$ Ser		6.40 ± 0.50	217 ± 50

K_M and K_i values were determined by a nonlinear fitting procedure from data of Fig. 1–3 and according to Eqs. 2 and 3, respectively.

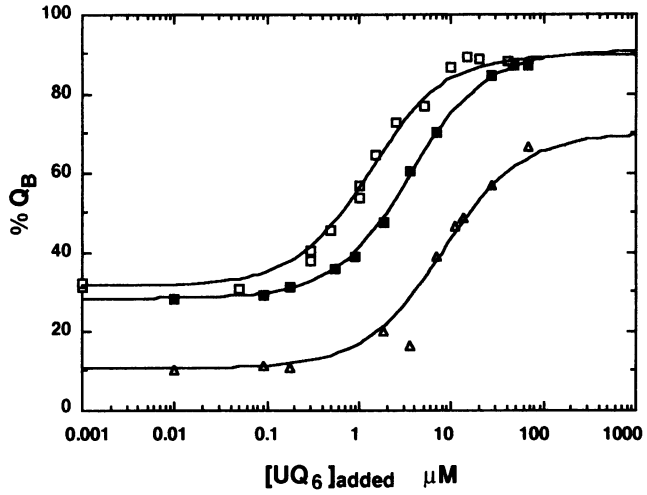

FIGURE 2 Quinone titrations (UQ_6) of the secondary quinone activity in reaction centers (~0.35 μM) from the wild type (■), the $Thr^{L226} \rightarrow$ Ala mutant (□), and the $Ile^{L229} \rightarrow$ Ser mutant (△). The lines result from a fitting procedure according to Eq. 2, with some modifications that account for the asymptotic value of $\%Q_B$ (see text). The dissociation constant obtained from this analysis are: for the wild type, K_M = 2.1 ± 0.3 μM; for the $Thr^{L226} \rightarrow$ Ala, K_M = 0.7 ± 0.15 μM; for the $Ile^{L229} \rightarrow$ Ser mutant, K_M = 6.4 ± 0.5 μM. Conditions as for Fig. 1.

and about 70% for $Ile^{L229} \rightarrow$ Ser. This probably arises from a lack of reconstitutibility of some fraction of the reaction centers. Therefore, in order to fit the data of Fig. 2 with Eq. 2, we have multiplied the right side of the equation by a factor that accounts for the asymptotic values of $\%Q_B$, mentioned above.

For simplification and because it does not significantly modify the estimated K_M values, we have neglected the differences between the dissociation constant values for UQ_6 and UQ_{10}. Thus, in Eq. 2, $[Q]_{total}$ represents $[UQ_6]_{added} + [UQ_{10}]_{residual}$. The results derived from those fittings are presented in Table 1. The derived K_M values for the wild type, $Thr^{L226} \rightarrow$ Ala and $Ile^{L229} \rightarrow$ Ser are 2.10 ± 0.30, 0.70 ± 0.15, and 6.40 ± 0.50 μM, respectively. It is of interest to note that, within the error bars, the ratio between the K_M values of the wild type and $Thr^{L226} \rightarrow$ Ala (2.1/0.7) for the UQ_6 titrations is close to that measured for the titrations of the UQ_{10} endogenous quinone (0.71/0.38).

The differences in the $K_M$values between the wild type and the $Thr^{L226} \rightarrow$ Ala mutant may result from steric reasons, the smaller side chain of Ala compared to Thr allowing a stronger binding of Q_B in $Thr^{L226} \rightarrow$ Ala.

Inhibitor binding affinities

K_i values for *o*-phenanthroline

The *o*-phenanthroline inhibition curves for the wild type, the $Thr^{L226} \rightarrow$ Ala and $Ile^{L229} \rightarrow$ Ser mutants are presented in Fig. 3. In order to calculate the dissociation constant values, K_i, for the three samples, we have fitted the curves with the model described in Eq. 3. This equation does not take into account the differences between free and total inhibitor concentrations. This is justified here since the *o*-phenanthroline concentrations used in the titration experiments are substantially greater than the reaction center concentrations. In other words, $[o\text{-phenanthroline}]_{total} \approx [o\text{-phenanthroline}]_{free}$.

$$\%Q_B = \frac{[Q]_{total}}{[Q]_{total} + K_M + \frac{K_M}{K_i} \times [I]_{total}} \quad (3)$$

In Eq. 3, $[I]_{total}$ represents the total inhibitor concentration. The $\%Q_B$ curves were obtained in samples containing a quinone concentration corresponding to 50% activity (Q_{50} values). Fitting the curves of Fig. 3 by Eq. 3 leads to the following K_i values: for the wild type, K_i = 166 ± 10 μM, for $Thr^{L226} \rightarrow$ Ala, K_i = 5 ± 2 μM, and for $Ile^{L229} \rightarrow$ Ser, K_i = 217 ± 50 μM (Table 1). The major observation is the greatly increased sensitivity toward *o*-phenanthroline of the $Thr^{L226} \rightarrow$ Ala mutant. In the $Ile^{L229} \rightarrow$ Ser mutant the K_i value is nearly unchanged compared to the wild type.

The terbutryn titration curves were also measured (data not shown) and lead to close I_{50} values for the three species (I_{50} = 9 ± 2 μM for the wild type, I_{50} = 4 ± 1 μM for $Ile^{L229} \rightarrow$ Ser, and I_{50} = 5 ± 1 μM for $Thr^{L226} \rightarrow$ Ala). Since the assumption made above for *o*-phenanthroline is not

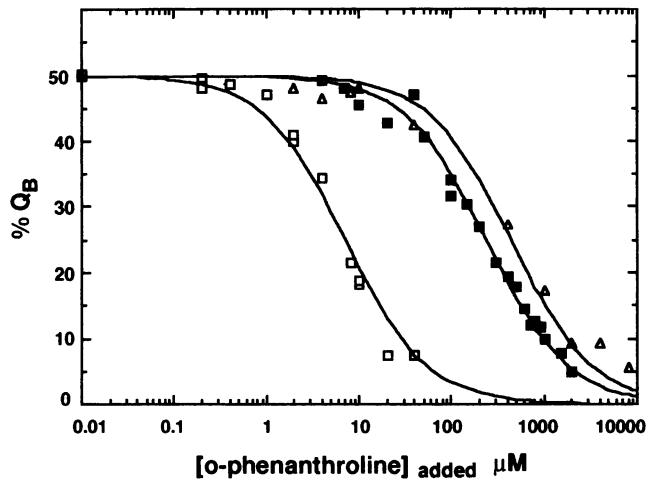

FIGURE 3 Secondary quinone activity (UQ_6) inhibition curves for *o*-phenanthroline in reaction centers from the wild type (■), the $Thr^{L226} \rightarrow$ Ala mutant (□), and the $Ile^{L229} \rightarrow$ Ser mutant (△). The lines are drawn by fitting the data with Eq.3. The derived dissociation constants for terbutryn are: for the wild type, K_i = 166 ± 10 μM; for the $Thr^{L226} \rightarrow$ Ala mutant, K_i = 5 ± 2 μM; for the $Ile^{L229} \rightarrow$ Ser mutant, K_i = 217 ± 50 μM. The reaction centers (0.9 μM) were suspended in sodium phosphate, 10 mM pH 7.5, LDAO 0.05%. T = 21°C. The initial quinone concentrations correspond to the Q_{50} values.

valid for terbutryn (I_{50} values ~$[RC]_{total}$), we did not quantitatively determined the K_i values for that inhibitor.

pH dependence of the $Q_A^- \leftrightarrow Q_B^-$ equilibrium constant

In order to calculate the pH titration curves of the $Q_A^- Q_B \leftrightarrow Q_A Q_B^-$ equilibrium constant (K_2), we have measured the pH dependence of the rate constants of $P^+Q_A^-$ and $P^+Q_B^-$ charge recombination (k_{AP} and k_{BP}, respectively) in the reaction centers from the wild type and the mutants.

$P^+Q_A^-$ charge recombination rates

The k_{AP} values were almost identical (within 5%) in the three strains, in the pH range 4–11.5. Therefore, we only present in Fig. 4 the k_{AP} pH dependence observed in the wild type. At pH 8, the lifetime of the $P^+Q_A^-$ charge recombination is about 120 ms, which is close to the value measured in *Rb. sphaeroides* reaction centers (12, 13). As observed in *Rb. sphaeroides*, a smooth regular pH dependence is observed in the pH range 4–11.5. This is probably accounted for by a direct route of charge recombination from the $P^+Q_A^-$ state in *Rb. capsulatus*.

$P^+Q_B^-$ charge recombination rates

The pH titrations of the $P^+Q_B^-$ charge recombination rate in the wild type and the $Thr^{L226} \rightarrow$ Ala and $Ile^{L229} \rightarrow$ Ser mutants are presented in Fig. 5.

The wild type. At pH 8, the lifetime of the $P^+Q_B^-$ charge recombination decay is equal to about 1.2 s. This is a value close to that measured in *Rb. sphaeroides* (13, 14). Applying the equation derived by Wraight (1): $K_2 + 1 = k_{AP}/k_{BP}$, suggests very close free energy gaps between the $P^+Q_A^-$ and $P^+Q_B^-$ states in the reaction centers from *Rb. capsulatus* and *Rb. sphaeroides*. This similarity is probably due to the similar quinone environment (due to the high sequence homology between the Q_B protein pockets of both species) and to the identical nature of the quinones (UQ_{10}) in both species. It is thus very probable that, in *Rb. capsulatus*, charge recombination from $P^+Q_B^-$ occurs, as in *Rb. sphaeroides* (14), via thermal repopulation of the $P^+Q_A^-$ state.

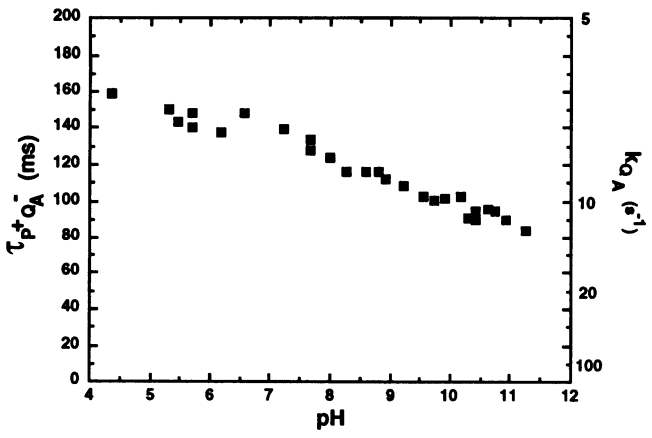

FIGURE 4 pH dependence of the lifetime of $P^+Q_A^-$ charge recombination measured at 865 nm, in reaction centers (~1 μM) from wild type *Rb. capsulatus* with low Q_B present. The reaction centers were suspended in LDAO 0.05%. For the different buffers see the Material and Methods section. T = 21°C.

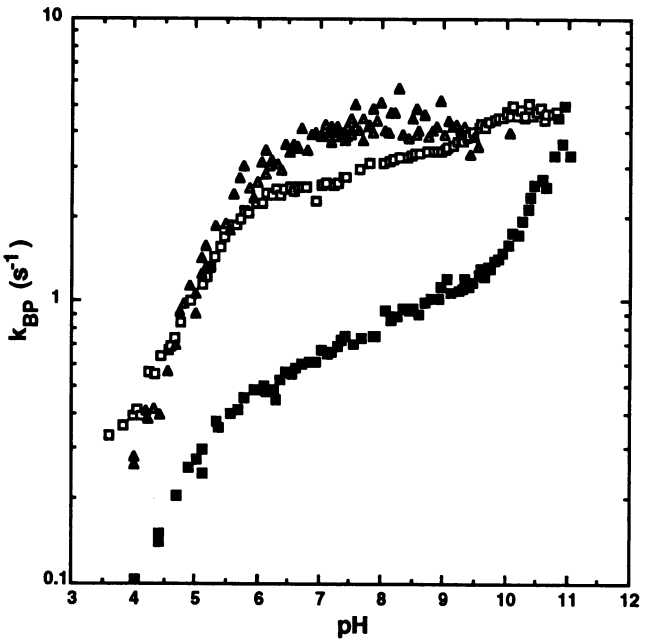

FIGURE 5 pH dependence of k_{BP}, the rate constant of $P^+Q_B^-$ charge recombination in the reaction centers (~1 μM) from the wild type (■), the $Thr^{L226} \rightarrow$ Ala mutant (□), and the $Ile^{L229} \rightarrow$ Ser mutant (▲). As mentioned in the text, for the $Ile^{L229} \rightarrow$ Ser and $Thr^{L226} \rightarrow$ Ala mutants, the rate constant of $P^+Q_A^-$ charge recombination (k_{AP}), which was independently measured, was fixed in the minimization program. This was done in order to prevent compensation effects between amplitudes and lifetimes values due to the low k_{AP}/k_{BP} ratio. Conditions as for Fig. 4.

Below pH 7, a substantial decrease of k_{BP} is observed going from 0.65 s^{-1} at pH 7 to about 0.1 s^{-1} at pH 4.

Above pH 10, a marked increase of k_{BP} occurs: $k_{BP} \approx 1.5$ s^{-1} at pH 10, and ≈ 5 s^{-1} at pH 11. In *Rb. sphaeroides*, the same behavior was observed for the wild type (14). However, a different pattern is displayed from *pH 7* to *pH 10* where, in *Rb. capsulatus* wild type, a smooth continuous increase of k_{BP} is detected.

The pH titration curve for K_2 is shown in Fig. 6. If only one protonation event occurs in the Q_B vicinity in the pH range where the curves are analyzed, one can describe the K_2 curves by the following equation:

$$K_2(\mathrm{pH}) = K_2^{H^+} \frac{1 + 10^{(\mathrm{pH} - \mathrm{pK}_{Q_A Q_B^-})}}{1 + 10^{(\mathrm{pH} - \mathrm{pK}_{Q_A^- Q_B})}} \qquad (4)$$

where $K_2^{H^+}$ represents the K_2 value at low pH, $pK_{Q_A Q_B^-}$ and $pK_{Q_A^- Q_B}$ are the pK values of the protonatable group close to Q_B when the electron is on Q_B and on Q_A, respectively. As pointed out by Takahashi and Wraight (13), this equation can be modified if direct interaction between this group and Q_A is assumed.

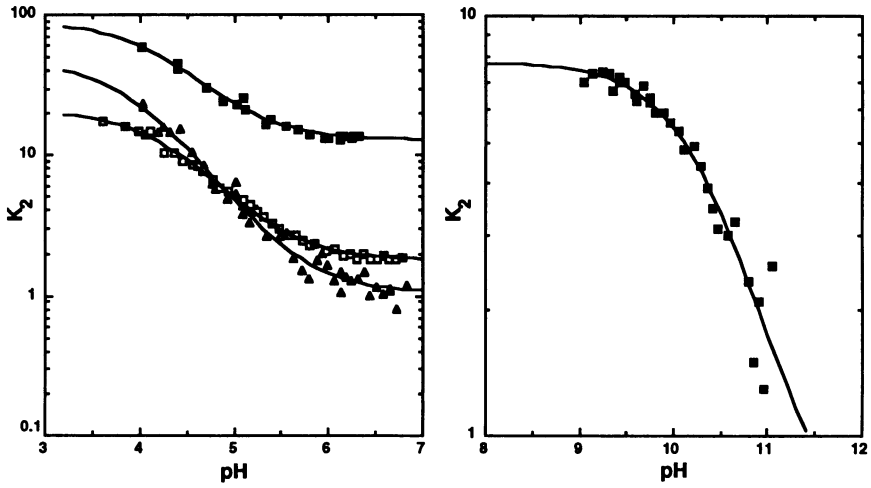

FIGURE 6 pH dependence of K_2, the $Q_A^- Q_B \leftrightarrow Q_A Q_B^-$ equilibrium constant, in the reaction centers from the wild type (■), the $Thr^{L226} \rightarrow$ Ala mutant (□), and the $Ile^{L229} \rightarrow$ Ser mutant (▲). The lines result from fitting the data with Eq. 4. The derived pK values for the Q_B and Q_B^- states are the following: for the wild type, $pK_{Q_A^- Q_B} = 4.2 \pm 0.2$ and $pK_{Q_A Q_B^-} = 5.1 \pm 0.1$ at low pH and $pK_{Q_A^- Q_B} = 10.3 \pm 0.1$ and $pK_{Q_A Q_B^-} = 11.6 \pm 0.3$, at high pH. For $Thr^{L226} \rightarrow$ Ala, $pK_{Q_A^- Q_B} \sim 4.3 \pm 0.2$ and $pK_{Q_A Q_B^-} \sim 5.2 \pm 0.1$; for $Ile^{L229} \rightarrow$ Ser, $pK_{Q_A^- Q_B} = 3.9 \pm 0.2$ and $pK_{Q_A Q_B^-} = 5.5 \pm 0.1$. Conditions as in Fig. 5.

The electrostatic interaction energy, ΔG_{int}, between the ionizable group and Q_B relates to $pK_{Q_A Q_B^-}$ and $pK_{Q_A^- Q_B}$:

$$\Delta G_{int} = \Delta pK \times 0.058 \text{ eV} \quad (5)$$

where $\Delta pK = pK_{Q_A Q_B^-} - pK_{Q_A^- Q_B}$

Fitting the K_2 curve, at low pH, for the wild type (Fig. 6, *left panel*) with Eq. 4 leads to $pKQ_A^- Q_B = 4.2 \pm 0.2$ and $pK_{Q_A^- Q_B} = 5.1 \pm 0.1$ (Table 2).

On the basis of data collected on *Rb. sphaeroides* mutants where Asp^{L213} was replaced by the nonprotonatable amino acid Asn, Takahashi and Wraight (15) have suggested that, in *Rb. sphaeroides*, the k_{BP} variations observed at low pH arise from deprotonation of Asp^{L213}. Because of the sequence homology existing between *Rb. sphaeroides* and *Rb. capsulatus* this is likely to be also the case in *Rb. capsulatus*.

The pK values calculated here for *Rb. capsulatus* are nearly the same as found for *Rb. sphaeroides* (13): 4 and 5, respectively. This suggests similar distance and environment (dielectric constant (ϵ)) between Asp^{L213} and Q_B^- in *Rb. capsulatus* and in *Rb. sphaeroides*. The ΔpK leads to an interaction energy between Asp^{L213} and Q_B^- of about 0.052 eV. Taking into account the measured distance between this amino acid and the quinone, in *Rb. sphaeroides* (~5.2 Å) (6), the local dielectric constant may be estimated as 53 ± 15. On the basis of data obtained in the T1 mutant ($Arg^{L217} \rightarrow$ His; $Ser^{L223} \rightarrow$ Ala) from *Rps. viridis*, we have previously calculated an ϵ value of 47 ± 15 between Arg^{L217} and Q_B^- (16).

TABLE 2 Apparent pK values derived from the pH dependence curves of K_2 in the wild type *Rb. capsulatus*, $Thr^{L226} \rightarrow$ Ala, and $Ile^{L229} \rightarrow$ Ser mutants

	Low pH		High pH	
	$pK_{Q_A^- Q_B}$	$pK_{Q_A Q_B^-}$	$pK_{Q_A^- Q_B}$	$pK_{Q_A Q_B^-}$
Wild type	4.2 ± 0.2	5.1 ± 0.1	10.3 ± 0.1	11.6 ± 0.3
$Thr^{L226} \rightarrow$ Ala	4.3 ± 0.2	5.25 ± 0.10		
$Ile^{L229} \rightarrow$ Ser	3.9 ± 0.2	5.5 ± 0.1		

These pK values were obtained by fitting the K_2 curves of Fig. 6 by a nonlinear fitting procedure according to Eq. 4.

These close estimations are in agreement with a similar and polar environment of the Q_B pocket.

The right panel of Fig. 6 presents the pH dependence of K_2 for the wild type at high pH. Fitting this curve with Eq. 4 leads to $pK_{Q_A Q_B^-}$ and $pK_{Q_A^- Q_B}$ values of 10.3 ± 0.1 and 11.6 ± 0.3, respectively (Table 2). If Glu^{L212} is responsible for these pK values in *Rb. capsulatus*, as suggested for the similar pK values found in *Rb. sphaeroides* by Paddock et al. (17), the above pK values lead to the determination of the local dielectric constant. Taking a value of 5.6 Å for the distance between Q_B and Glu^{L212} from the structure of *Rb. sphaeroides* (18), ϵ may be estimated to 34 ± 10, which is still a relatively high value.

However, the apparent pK values measured above at low and high pH may not be due to the only Asp^{L213} and Glu^{L212}, respectively, but rather to the overall influence of more than one amino acid (19). Therefore, the above ϵ values must be considered only as rough estimations.

The $Ile^{L229} \rightarrow$ Ser mutant. As displayed in Fig. 5, a substantial destabilization of Q_B^- occurs in this mutant compared to the wild type *Rb. capsulatus*.

From pH 7 to 10, k_{BP} is nearly constant and equal to about 4.5 s^{-1}. This value is close to that measured, at pH 8, in the IM(L229) mutant from *Rb. sphaeroides* (4). At pH 9, k_{AP} equals about 10 s^{-1} in $Ile^{L229} \rightarrow$ Ser, leading to a k_{AP}/k_{BP} ratio of about 2. According to the equation derived by Wraight (1), this reflects very close free energy levels for the $P^+Q_A^-$ and $P^+Q_B^-$ charge-separated states in this mutant.

Above pH ~10, k_{BP} remains constant (~4.5 s^{-1}) at variance to the wild type which displays a substantial increase of this parameter above pH 10. In addition, *above pH 10.2*, the amplitude of the slow phase of charge recombination becomes very small, suggesting a very weak binding of Q_B. It was thus impossible to further titrate k_{BP} at high pH. The weaker binding of Q_B was verified by monitoring the amount of cytochrome c_2 oxidation (550 nm) after the second flash relative to the first one (data not shown).

To analyze our data, we used a nonlinear Marquardt algorithm. In the wild type, k_{BP} and k_{AP} are sufficiently distinct

to allow a two-exponential decomposition, without fixing k_{AP}. This is not the case in the Ile^{L229} → Ser mutant. If we do not fix k_{AP} in the mutant, compensation effects between the lifetimes and the amplitudes of the two components make the decomposition analysis impossible. When k_{AP} is fixed (to its value measured independently in the low Q_B reaction center preparation), k_{BP} does not increase, at least up to pH 10.2. This observation disagrees with the continuous k_{BP} increase observed by Paddock et al. (4) in the IM(L229) mutant from *Rb. sphaeroides*. Part of this disagreement probably originates from neglecting these mathematical effects in the data of Paddock et al.

In the pH range 4–7, a similar protonation event as in the wild type leads to a decrease of k_{BP} in the Ile^{L229} → Ser mutant, from about 4.5 s^{-1} at pH 7 to 0.25 s^{-1} at pH 4. Using the k_{AP} values displayed in Fig. 4 for the wild type, the pH dependence curve of K_2 shown in the left panel of Fig. 6 is obtained. Using Eq. 4 to fit these low pH data gives $pK_{Q_A^- Q_B} = 3.9 \pm 0.2$ and $pK_{Q_A Q_B^-} = 5.5 \pm 0.1$ (Table 2). These figures are close to those derived from the wild type data. The slight increase of ΔpK may result from small changes in the local dielectric constant and/or the distance between Asp^{L213} and Q_B.

The Thr^{L226} → Ala mutant. The pH titration curve of k_{BP} for this mutant is presented in Fig. 5. As discussed below, the increased binding affinity for Q_B (UQ_6 and UQ_{10}) compared to the wild type is consistent with the observed destabilization of the free energy level of $P^+Q_B^-$ (higher k_{BP}) in this mutant. The pattern of k_{BP} variations is nearly the same as in the wild type but with a smoother amplitude at high pH.

At low pH (3.5–7) a strong dependence is observed: $k_{BP} \approx 0.33$ s^{-1} at pH 3.5 and $k_{BP} \approx 2.5$ s^{-1} at pH 7. The pH dependence of K_2 in Thr^{L226} → Ala is presented in the left panel of Fig. 6. Fitting of this curve by Eq. 4 leads to $pK_{Q_A^- Q_B} \sim 4.3 \pm 0.2$ and $pK_{Q_A Q_B^-} \approx 5.25 \pm 0.1$ (Table 2). These values are in good agreement with those derived from the wild type, suggesting that no major change happened in the tertiary structure of the L subunit in the vicinity of Asp^{L213} nor in its distance from Q_B.

In the pH range 7–9, a slight continuous increase of k_{BP} is displayed from 2.5 s^{-1} at pH 7 to about 3.3 s^{-1} at pH 9.

In the pH range 9–10 an increase of k_{BP} is observed reaching a value of about 4.5 s^{-1} and stays constant above pH 10. This upper value of $k_{BP} \approx 0.5\ k_{AP}$ is similar to that observed in the Ile^{L229} → Ser mutant, and corresponds to close free energy levels of $P^+Q_A^-$ and $P^+Q_B^-$ states. At variance to the Ile^{L229} → Ser mutant, above pH 10, the Q_B binding affinity in Thr^{L226} → Ala did not vary (as indicated by monitoring cytochrome oxidation at 550 nm on the second flash relative to the first flash).

Q_A^- → Q_B electron transfer rates

In order to correlate the energetics and the kinetics processes of the quinone system, we have also measured the rate constants of electron transfer from Q_A^- to Q_B (k_{AB}) in Thr^{L226} → Ala, Ile^{L229} → Ser, and wild type *Rb. capsulatus* reaction centers. These measurements were done at 750 nm as previously reported for *Rb. sphaeroides* (20), using the apparatus described in Ref. 21. The kinetics are presented in Fig. 7. The absence of absorbance change increase in the presence of terbutryn (Fig. 7) is consistent with the attribution of the observed kinetics to the electron transfer process from Q_A^- to Q_B. At pH 7, we found $k_{AB} = (65 \pm 10\ \mu s)^{-1}$ for the wild type, $(65 \pm 10\ \mu s)^{-1}$ for the Thr^{L226} → Ala mutant and $(180 \pm 20\ \mu s)^{-1}$ for the Ile^{L229} → Ser mutant. k_{AB} for the wild type is notably faster than in wild type *Rb. sphaeroides* ($(\sim 200\ \mu s)^{-1}$ (13, 21)). Marcus theory (23) suggests for k_{AB} the following equation:

$$k_{AB} = A \times e^{-((\Delta G^o + \lambda)^2/4\lambda kT)} \quad (6)$$

where A is a constant depending on the probability of penetration of the electron through the energy barrier of the reaction and on the distance between the reactants. ΔG^o is the free energy gap between the states $P^+Q_A^-$ and $P^+Q_B^-$. λ is the reorganization energy of the solvent and protein environment around the electron carriers. As a consequence of the close similarities between the quinone system as well as between the Q_A and Q_B protein pockets in *Rb. capsulatus* and in *Rb. sphaeroides*, ΔG^o is nearly the same in both species. That is readily concluded from the close values of k_{AP} and k_{BP} in the two species, respectively. The differences of k_{AB} values in the two species may arise from small differences in the reorganization energies between the two types of reaction centers or reflect a difference in the A factor. A smaller $Q_A - Q_B$ distance in *Rb. capsulatus* compared to *Rb.*

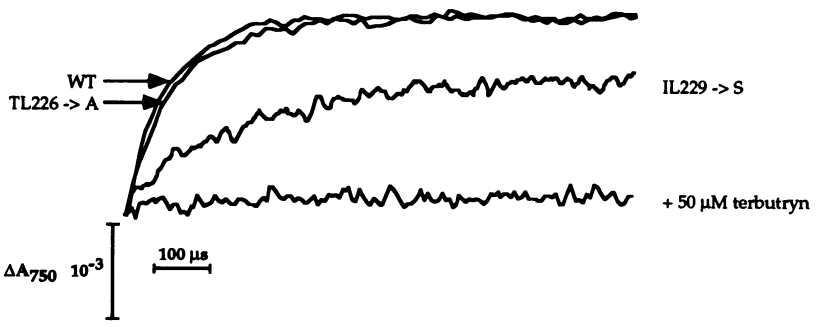

FIGURE 7 Kinetics of Q_A^- → Q_B electron transfer measured at 750 nm in the reaction centers (2 µM) from *Rb. capsulatus* wild type and the Thr^{L226} → Ala and Ile^{L229} → Ser mutants. These curves were obtained using the electrochromic band shift of the bacteriopheophytin (20). The kinetics were accumulated four times. The reaction centers were suspended in bis-Tris propane, 10 mM, pH 7, LDAO 0.05%.

sphaeroides could account for a higher k_{AB} value in the former species. Assuming that (i) λ is unchanged for the electron transfer reaction between the wild type and the mutants; (ii) $\delta\Delta G^o$ and ΔG^o are much smaller than λ, Paddock et al. (4) have suggested that if ΔG^o is changed by $\delta\Delta G^o$ in a mutant, the rate constant (k'_{AB}) of electron transfer in the mutant will be related to k_{AB} of the wild type as follows:

$$k'_{AB} = k_{AB} \times e^{-(\delta\Delta G^o/2kT)} \quad (7)$$

In *Rb. sphaeroides*, this equation was satisfactory in describing the differences observed in the k_{AB} values between the wild type and the IM(L229) mutant, but failed when it was applied to the YG(L222) mutant (24).

Here, in *Rb. capsulatus*, at pH 7, a $\delta\Delta G^o$ value of about −60 meV may be estimated between the wild type and the $Ile^{L229} \rightarrow$ Ser mutant, on the basis of their respective K_2 values (Fig. 6). This roughly corresponds to the calculated k_{AB}/k'_{AB} ratio of about 3 according to Eq. 7. However, the correspondence is not good when k'_{AB} for $Thr^{L226} \rightarrow$ Ala is compared to k_{AB} for the wild type. At pH 7, K_2 for $Thr^{L226} \rightarrow$ Ala is about 1.7, resulting in a ΔG° value of about −13 meV. Therefore, $\delta\Delta G^\circ$ between the $Thr^{L226} \rightarrow$ Ala mutant and the wild type is about 47 meV. According to Eq. 7, one would expect k_{AB}/k'_{AB} to be about 2.5 which disagrees with the measured ratio of ~1.

Thus, the assumptions made in Eq. 7 could only be valid when applied to mutants at L229. In other mutants, as $Thr^{L226} \rightarrow$ Ala, Q_B may be bound in a different conformation, potentially resulting in either a change in the reorganization energy and/or the distance between Q_A and Q_B relative to the wild type. A slight decrease of the distance between Q_A and Q_B could fortuitously balance the expected decrease of k'_{AB} due to the smaller ΔG^o in the $Thr^{L226} \rightarrow$ Ala mutant compared to the wild type.

DISCUSSION

We have analyzed the reaction centers from wild type *Rb. capsulatus* and two mutants, $Thr^{L226} \rightarrow$ Ala and $Ile^{L229} \rightarrow$ Ser, in terms of Q_B and herbicides binding affinities and the pH dependencies of the equilibrium constant K_2.

By diluting the reaction center preparations from the wild type and $Thr^{L226} \rightarrow$ Ala, we were able to obtain an approximate estimation of the dissociation constant for native Q_B. The 2–3-fold increase of the native UQ_{10} affinity for the Q_B pocket compared to UQ_6 observed in both types of reaction centers agrees reasonably well with the results of McComb et al. (25) who found in wild type *Rb sphaeroides* reaction centers dissociation constants of 1.7 and 4 μM for UQ_{10} and for UQ_6, respectively. This suggests that the parameters controlling Q_B binding are likely to be the same in *Rb. sphaeroides* and in *Rb. capsulatus*.

The high sensitivity to *o*-phenanthroline of $Thr^{L226} \rightarrow$ Ala compared to the wild type *Rb. capsulatus* is similar to that observed in *Rps. viridis*, where Ala is naturally in position L226. In *Rps. viridis*, I_{50}/Q_{50} ratios of 4 (26) and 6.5 (27) were obtained, close to the value of 8.5 measured here in $Thr^{L226} \rightarrow$ Ala. In contrast, these ratios are about 125 in *Rb. capsulatus* wild type (this work) and about 240 in *Rb. sphaeroides* (4). Thr^{L226} is conserved in all purple bacteria which have been sequenced, except in *Rps. viridis*. Taking into account the similar sensitivity to *o*-phenanthroline in wild type *Rps viridis* and in $Thr^{L226} \rightarrow$ Ala, we propose that the residue in position L226 has an important role in the binding of that inhibitor. From the three-dimensional structure of *Rps. viridis* reaction centers crystallized in the presence of *o*-phenanthroline, the distance between the β carbon of Ala^{L226} and the closest ring of *o*-phenanthroline is 3.9 Å (I. Sinning, personal communication). This distance is at the upper limit to allow van der Waals contacts between Ala^{L226} and *o*-phenanthroline. It is therefore likely that the much lower affinity for *o*-phenanthroline in wild type *Rb. sphaeroides* and *Rb. capsulatus* is due to steric effects of the larger Thr side chain which prevents *o*-phenanthroline from making other interactions in the Q_B pocket. The $Thr^{L226} \rightarrow$ Ala mutation would mimic the Q_B pocket of *Rps. viridis*, especially at the connection of the transmembrane helix E and the helix de. Alternatively, it is possible that the binding sites for *o*-phenanthroline are structurally different in *Rb. capsulatus* and *Rps. viridis*, with "low" and "high" affinities, respectively. By analogy with *Rb. sphaeroides*, in *Rb. capsulatus*, Thr^{L226} may contract an hydrogen bond which is important for the tertiary structure of that region of the protein. Disruption of that bond upon replacement of Thr, could favor a structural change leading to a "high" affinity binding site for *o*-phenanthroline. Structural information from *Rb. sphaeroides* binding *o*-phenanthroline would be useful to check this hypothesis.

The $Ile^{L229} \rightarrow$ Ser mutant was previously found to be much more terbutryn-sensitive that the wild type (9). We show here that this does not only originate from sensitivity toward terbutryn of the reaction centers, but also from a higher dissociation constant of the quinone in the reaction center mutant than in the wild type.

pH dependencies of $P^+Q_B^-$ charge recombination kinetics in $Thr^{L226} \rightarrow$ Ala and $Ile^{L229} \rightarrow$ Ser display substantial destabilization of the semiquinone, relatively to the wild type. As noted by Shopes and Wraight (26), the midpoint redox potential (E_m) value for the couple Q_B/Q_B^- reflects the differential binding affinities for Q_B and Q_B^-. The lower E_m value (higher $P^+Q_B^-$ free energy level) measured in $Thr^{L226} \rightarrow$ Ala compared to the wild type, together with the finding of a higher binding affinity for Q_B in $Thr^{L226} \rightarrow$ Ala implies that the semiquinone form is not more tightly bound. This is not seen in the $Ile^{L229} \rightarrow$ Ser mutant where the K_M value is higher than in the wild type. We thus have to postulate that, in $Ile^{L229} \rightarrow$ Ser, Q_B^- binding is decreased compared to the wild type, further than is Q_B binding. In other words, the relative decrease binding affinity observed in $Ile^{L229} \rightarrow$ Ser is even more pronounced when the semiquinone is formed. This could arise from an unfavorable electrostatic interaction between the negative charge present on the semiquinone and the partial negative charge carried by the side chain of serine.

Rb. capsulatus reaction centers have not yet been crystallized. On the basis of the high homology of their primary sequence, it is generally assumed that the physical and spectroscopic properties of the reaction centers are essentially the same in both strains. However, in the present work, we show that notable differences exist between the two types of reaction centers. In wild type *Rb. capsulatus* reaction centers, we have measured a Q_A^- to Q_B electron transfer rate three times higher than in *Rb. sphaeroides*. Since ΔG^o is about the same in both species, and if we assume that the reorganization energy λ is also the same, it could be that Q_A and Q_B are slightly closer in *Rb. capsulatus*. Moser et al. (28) have recently proposed that, in proteins, the edge-to-edge distance (d (Å)) between electron carriers is the main factor governing the maximal electron transfer rate. These authors have suggested an $e^{-1.4.d}$ dependence factor of the maximal rate in proteic systems. According to that model, Q_A and Q_B should be about 0.7 Å closer in *Rb. capsulatus* than in *Rb. sphaeroides*.

The pH dependence curves of k_{BP} in the wild type *Rb. capsulatus* also display differences with *Rb. sphaeroides*. In the pH range 7–10 a twofold increase of k_{BP} is observed in *Rb. capsulatus*, whereas, in *Rb. sphaeroides*, k_{BP} remains constant in the same pH range. In the close environment of Q_B, only a few differences exist between the primary sequences concerning the protonatable amino acids in both strains. Tyr^{L215} is the only protonatable amino acid present in the Q_B binding pocket of *Rb. capsulatus* which corresponds to a nonprotonatable residue in *Rb. sphaeroides* (Phe^{L215}). We therefore think that, in the pH range 7–10, the observed increase of k_{BP} in *Rb. capsulatus* may be due to deprotonation of Tyr^{L215}. Changing Tyr^{L215} to Phe in the reaction centers from *Rb. capsulatus* could help to test whether this residue is involved in the above effect. It is also possible that the different pH behavior of k_{BP} in *Rb. capsulatus* and *Rb. sphaeroides* results from a different overall charge distribution in the Q_B binding pocket. This would exhibit an apparent pK in *Rb. capsulatus*, that already exists in *Rb. sphaeroides* but at a very different pH or which is screened because of a higher polarity in that region of the protein. This may reflect slight differences in the structures of the reaction centers from *Rb. capsulatus* and *Rb. sphaeroides*.

Dr. Paul Mathis is acknowledged for his collaboration in the measurements of the $Q_A^- \rightarrow Q_B$ electron transfer rates. The authors are pleased to thank Drs. B. Arnoux, F. Haraux, J. Lavergne, and C. Vernotte for helpful discussions, Drs. W. Liebl and A. W. Rutherford for careful reading of the manuscript, and I. Sinning for communicating structural informations about *Rps. viridis* reaction center. M. C. Gonnet is thanked for her technical assistance in the wild type and mutants cells growth.

REFERENCES

1. Wraight, C. A. 1981. Oxidation-reduction physical chemistry of the acceptor quinone complex in bacterial photosynthetic reaction centers: evidence for a new model of herbicide activity. *Isr. J. Chem.* 21:348–354.
2. McPherson, P. H., M. Y. Okamura, and G. Feher. 1990. Electron transfer from the reaction center of *Rb. sphaeroides* to the quinone pool: doubly reduced Q_B leaves the reaction center. *Biochim. Biophys. Acta*. 1016: 289–292.
3. Bylina, E. J., and D. C. Youvan 1987. Genetic engineering of herbicide resistance: saturation mutagenesis of Isoleucine 229 of the reaction center L subunit. *Z. Naturforsch.* 42c:769–774.
4. Paddock, M. L., S. H. Rongey, E. C. Abresch, G. Feher, and M. Y. Okamura. 1988. Reaction centers from three herbicide-resistant mutants of *Rhodobacter sphaeroides* 2.4.1.: sequence analysis and preliminary characterization. *Photosynt. Res.* 17:75–96.
5. Sinning, I., and H. Michel. 1987. Sequence analysis of mutants from *Rhodopseudomonas viridis* resistant to the herbicide terbutryn. *Z. Naturforsch.* 42c:751–754.
6. Allen, J. P., G. Feher, T. O. Yeates, H. Komiya, and D. C. Rees. 1988. Structure of the reaction center from *Rhodobacter sphaeroides* R-26: protein-cofactor (quinone and Fe^{2+}) interactions. *Proc. Natl. Acad. Sci. USA*. 85:8487–8491.
7. Chang, C. H., O. El-kabanni, D. Tiede, J. Norris, and M Schiffer. 1991. Structure of the membrane-bound protein photosynthetic reaction center from *Rhodobacter sphaeroides*. *Biochemistry*. 22:5353–5360.
8. El-kabanni, O., C. H. Chang, D. Tiede, J. Norris, and M. Schiffer. 1991. Comparison of reaction centers from *Rhodobacter sphaeroides* and *Rhodopseudomonas viridis*: overall architecture and protein-pigment interactions. *Biochemistry*. 30:5361–5369.
9. Bylina, E. J., R. V. M. Jovine, and D. C. Youvan. 1989. A genetic system for rapidly assessing herbicides that compete for the quinone binding site of photosynthetic reaction centers. *Biotechnology*. 7:69–74.
10. Michel, H., O. Epp, and J. Deisenhofer. 1986. Pigment-protein interactions in the photosynthetic reaction centre from *Rhodopseudomonas viridis*. *EMBO J.* 10:2445–2451.
11. Gast, P., T. J. Michalski, J. E. Hunt, and J. R. Norris. 1985. Determination of the amount and type of quinones present in single crystals from reaction center protein from the photosynthetic bacterium *Rhodopseudomonas viridis*. *FEBS Lett.* 2:325–328..
12. Feher, G., T. R. Arno, and M. Y. Okamura. 1988. The effect of an electric field on the charge recombination rate of $D^+Q_A^- \rightarrow DQ_A$ in reaction centers from *Rhodobacter sphaeroides* R-26. *In* The Photosynthetic Bacterial Reaction Center: Structure and Dynamics. J. Breton and A. Verméglio, editors. Plenum Press, New York. 271–287.
13. Takahashi, E., and C. A. Wraight. 1992. Proton and electron transfer in the acceptor quinone complex of *Rhodobacter sphaeroides*: characterization of site-directed mutants of the two ionizable residues, Glu^{L212} and Asp^{L213}, in the Q_B binding site. *Biochemistry*. 31:855–866.
14. Kleinfeld, D., M. Y. Okamura, and G. Feher. 1984. Electron transfer in reaction centers of *Rhodobacter sphaeroides*. I Determination of the charge recombination pathway of $D^+Q_AQ_B^-$ and free energy and kinetic relations between $Q_A^-Q_B$ and $Q_AQ_B^-$. *Biochim. Biophys. Acta*. 766: 126–140.
15. Takahashi, E., and C. A. Wraight. 1990. A crucial role for Asp^{L213} in the proton pathway to the secondary quinone of reaction centers from *Rb. sphaeroides*. *Biochim. Biophys. Acta*. 1020:107–111.
16. Baciou, L., I. Sinning, and P. Sebban. 1991. Study of Q_B^- stabilization in herbicide-resistant mutants from the purple bacterium *Rhodopseudomonas viridis*. *Biochemistry*. 37:9110–9116.
17. Paddock, M. L., S. H. Rongey, G. Feher, and M. Y. Okamura. 1989. Pathway of proton transfer in bacterial reaction centers: replacement of glutamic acid 212 in the L subunit by glutamine inhibits quinone (secondary acceptor) turnover. *Proc. Natl. Acad. Sci. USA*. 86:6602–6606.
18. Okamura, M. Y., and Feher, G. 1992. Proton transfer in reaction centers from photosynthetic bacteria. *Annu. Rev. Biochem.* 61:861–896.
19. Hanson, D. K., L. Baciou, D. M. Tiede, S. L. Nance, M. Schiffer, and P. Sebban. 1992. In bacterial reaction centers protons can diffuse to the secondary quinone by alternative pathways. *Biochim. Biophys. Acta*. 1102:260–265.
20. Vermeglio, A., T. Martinet, and R. K. Clayton. 1982. Mode of inhibition of electron transport by orthophenanthroline in chromatophores and reaction centers of *Rhodopseudomonas sphaeroides*. *Proc. Natl. Acad. Sci. USA*. 4:1809–1813..
21. Mathis, P., I. Sinning, and H. Michel. 1992. Kinetics of electron transfer from the primary to the secondary quinone in *Rhodopseudomonas viridis*. *Biochim. Biophys. Acta* 1098:151–158.

22. Vermeglio, A., and R. K. Clayton. 1977. Kinetics of electron transfer between the primary and the secondary electron acceptor in reaction centers from *Rhodopseudomonas sphaeroides*. *Biochim. Biophys. Acta* 461:159–164.
23. Marcus, R. A., and N. Sutin. 1985. Electron transfer in chemistry and biology. *Biochim. Biophys. Acta*. 811:265–322.
24. Paddock, M. L., G. Feher, and M. Y. Okamura. 1991. Reaction centers from three herbicide resistant mutants of Rhodobacter sphaeroides 2.4.1: kinetics of electron transfer reactions. *Photosynt. Res.* 27:109–119.
25. McComb, J. C., R. R. Stein, and C. A. Wraight. 1990. Investigations on the influence of headgroup substitution and isoprene side-chain length in the function of primary and secondary quinones of bacterial reaction centers. *Biochim. Biophys. Acta*. 1015:156–171.
26. Shopes, R. J., and C. A. Wraight. 1987. Herbicide-resistant reaction center mutants of *Rhodopseudomonas viridis*. *In* the proceedings of the VII[th] International Congress on Photosynthesis. J. Biggins, editor. Martinus Nijhoff/Holland. 397–400.
27. Sinning, I., H. Michel, P. Mathis, and A. W. Rutherford. 1989. Characterization of four herbicide-resistant mutants of *Rhodopseudomonas viridis* by genetic analysis, electron paramagnetic resonance, and optical spectroscopy. *Biochemistry*. 28:5544–5553.
28. Moser, C. C., J. M. Keske, K. Warncke, R. S. Farid, and P. L. Dutton. 1992. Nature of biological electron transfer. *Nature*. 355:796–802.